JOURNAL OF VIROLOGY, Nov. 2005, p. 13673–13684 Vol. 79, No. 21
0022-538X/05/$08.00+0 doi:10.1128/JVI.79.21.13673–13684.2005

Influenza Virus Hemagglutinin (H3 Subtype) Requires Palmitoylation of Its Cytoplasmic Tail for Assembly: M1 Proteins of Two Subtypes Differ in Their Ability To Support Assembly

Benjamin J. Chen,[1] Makoto Takeda,[1,2]† and Robert A. Lamb[1,2]*

Department of Biochemistry, Molecular Biology, and Cell Biology,[1] and Howard Hughes Medical Institute,[2] Northwestern University, Evanston, Illinois 60208-3500

Received 5 May 2005/Accepted 11 August 2005

The influenza A virus hemagglutinin (HA) transmembrane domain boundary region and the cytoplasmic tail contain three cysteines (residues 555, 562, and 565 for the H3 HA subtype) that are highly conserved among the 16 HA subtypes and which are each modified by the covalent addition of palmitic acid. Previous analysis of the role of these conserved cysteine residues led to differing data, suggesting either no role for HA palmitoylation or an important role for HA palmitoylation. To reexamine the role of these residues in the influenza virus life cycle, a series of cysteine-to-serine mutations were introduced into the HA gene of influenza virus A/Udorn/72 (Ud) (H3N2) by using a highly efficient reverse genetics system. Mutant viruses containing HA-C562S and HA-C565S mutations had reduced growth and failed to form plaques in MDCK cells but formed wild-type-like plaques in an MDCK cell line expressing wild-type HA. In cell-cell fusion assays, nonpalmitoylated H3 HA, in both cDNA-transfected and virus-infected cells, was fully competent for HA-mediated membrane fusion. When the HA cytoplasmic tail cysteine mutants were examined for lipid raft association, using as the criterion Triton X-100 insolubility, loss of raft association did not show a direct correlation with a reduction in virus replication. However, mutant virus assembly was reduced in parallel with reduced virus replication. Additionally, a reassortant of strain A/WSN/33 (WSN), containing the Ud HA gene with mutations C555S, C562S, and C565S, produced virus that could form plaques on regular MDCK cells and had only moderately decreased replication, suggesting differences in the interactions between Ud and WSN HA and internal viral proteins. Analysis of M1 mutants containing substitutions in the six residues that differ between the Ud and WSN M1 proteins indicated that a constellation of residues are responsible for the difference between the M1 proteins in their ability to support virus assembly with nonpalmitoylated H3 HA.

Influenza virus acquires a lipid envelope by budding from the apical surface of virus-infected cells (25). Two major spike glycoproteins, hemagglutinin (HA) and neuraminidase (NA), are incorporated into the virus envelope during budding, together with much lesser amounts of the M2 proton-selective ion channel protein (18). The influenza virus HA glycoprotein plays at least three major roles in the virus life cycle: (i) HA binds to sialic acid-containing receptors on the cell surface, (ii) HA is responsible for the penetration of the virus into the cell cytoplasm by mediating low pH-induced fusion between the virus and endosomal membranes, and (iii) HA is the major viral antigen against which neutralizing antibodies are generated (18).

Whereas the atomic structures of HA of differing subtypes indicate very similar architectures overall, the 16 subtypes of HA at the amino acid level range in similarity from 30 to 70% (28). However, three cysteine residues in the HA cytoplasmic tail region are well conserved among the 16 HA subtypes (28). For the H3 subtype, these cysteines are at position 555, located at the border between the transmembrane (TM) domain and cytoplasmic tail, and positions 562 and 565, which reside in the cytoplasmic tail. Each of the three cysteine residues is modified posttranslationally by the addition of palmitic acid through a thioether linkage (15, 23, 42, 45). Mutagenesis studies, in which each of the three conserved cysteine residues was substituted with alanine (15) or serine (42), suggest that the extent of palmitate addition changes with each mutant, i.e., palmitoylation is a moving target. For some cellular proteins, e.g., the T-cell adaptor protein LAT (11), the B-cell tetraspanin CD81 (7), and several Src family kinases (16), the addition of palmitate is thought to be essential for targeting these proteins to lipid raft domains (22). Lipid raft microdomains are dynamic structures on cell surfaces that are enriched in cholesterol and sphingolipids and are assumed to function as selective concentration devices for proteins and to serve as platforms for signal transduction (40). In addition, it has been shown that several enveloped viruses, including influenza virus (36, 43), Ebola virus (3), and human immunodeficiency virus type 1 (HIV-1) (29), assemble and bud from lipid raft-like domains.

Mutagenesis studies indicated that HA palmitoylation is not required for HA biosynthesis or HA intracellular transport (23, 41, 42). However, the role of palmitoylation in HA-mediated membrane fusion appears to vary dramatically among different HA subtypes. An analysis of H2 subtype HA cysteine mutants indicated that in HA-expressing cells, low pH-induced membrane fusion did not occur (23). Although, subsequent analogous studies using HA-expressing systems failed to

* Corresponding author. Mailing address: Department of Biochemistry, Molecular Biology, and Cell Biology, Northwestern University, 2205 Tech Dr., Evanston, IL 60208-3500. Phone: (847) 491-5433. Fax: (847) 491-2467. E-mail: ralamb@northwestern.edu.

† Present address: Faculty of Medicine, Kyushu University, Fukuoka, Japan.

support these findings not only for H2 subtype HA (24) but also for the H3 (15, 21, 41, 42) and H7 (30, 45) subtypes. These later studies indicated that palmitoylation was not required for HA-mediated fusion as judged by syncytia formation, fluorescence dequenching, and dye transfer assays. On the other hand, studies in which the conserved cysteine residues of the H1 HA were mutated have shown that removal of the palmitoylation sites from vector-expressed HA restricts fusion at the step of pore formation (34). Moreover, for H7 HA, recent observations on dye transfer between virus-infected cells and red blood cells (RBCs) show that palmitoylation of H7 HA has a role in promoting efficient fusion in the context of virus infection (46). In none of these studies is a cysteine residue per se considered important for HA function, as various residues have been substituted for cysteine (e.g., alanine, serine, proline, tyrosine, and methionine) (15, 21, 23, 41, 42, 53).

Considerable evidence exists that in addition to a subtype-dependent role of HA cytoplasmic tail palmitoylation in HA-mediated fusion, the HA cytoplasmic tail is multifunctional and controls, directly or indirectly, virus morphology (14) and genome packaging (50) and promotes membrane association of M1 (1, 9). Furthermore, another step in the virus life cycle that may require HA palmitoylation is the step of virus assembly, particularly as the localization of HA to lipid raft microdomains is essential for efficient virus budding (43). A role for palmitoylation in virus assembly was first suggested when cysteine substitutions were made in A/WSN/33 (WSN) HA (H1), resulting in the rescue of altered virus by using the original influenza virus reverse genetics system (53). Mutations at the cysteine residue equivalent to H3-C562 led to highly attenuated viruses, and mutations at the cysteine residue equivalent to H3-C565 failed to yield infectious particles (53). When similar mutations were introduced into A/Udorn/72 (Ud) HA (H3) and viruses recovered within a WSN genetic background (WSN7+Ud HA), the replication of palmitoylation-deficient viruses in both tissue culture and mice was somewhat attenuated when cysteine residues 562 and 565 were mutated individually. However, HA mutants containing two or more cysteine-to-alanine mutations could not be rescued as viable virus (15). The original virus recovery system may have limited the rescue of severely debilitated viruses. This obstacle has also been encountered when using the newer highly efficient reverse genetics system. When attempts to rescue A/FPV/Rostock/34 (H7) carrying multiple HA cysteine residue mutations were made, only single cysteine-to-serine HA mutant viruses could be recovered (46). These studies demonstrated that HA palmitoylation is important in the virus life cycle, particularly as revertant viruses could be recovered that restored cysteine residues (15). The mechanism by which palmitoylation contributes to virus replication and whether this is related to lipid raft localization and/or virus assembly remain unclear.

In this study, we generated cysteine-to-serine mutations in H3 HA and determined how these mutations affected both vector-expressed HA and recovered virus. Our results show that palmitoylation is dispensable for H3 HA-mediated membrane fusion. In the context of Ud virus, however, palmitoylation is required for virus assembly and thus is required for efficient virus replication.

MATERIALS AND METHODS

Cells and viruses. Madin-Darby canine kidney (MDCK) cells, 293T cells, HeLa T4 cells, and CV1 cells were maintained in Dulbecco's modified Eagle's medium (DMEM) supplemented with 10% fetal bovine serum (FBS). Baby hamster kidney (BHK) cells were maintained in DMEM supplemented with 10% FBS and 10% tryptose phosphate broth. MDCK-HA cells stably expressing the influenza virus Ud HA have been described previously (43). All cells were maintained in a humidified incubator at 37°C with 5% CO_2. Wild-type (wt) and mutant influenza A viruses (Ud and WSN genetic backbones) were generated by reverse genetics from cDNAs essentially as described previously (26). Briefly, 293T cells were transfected with eight genome-sense plasmids along with four protein-expressing plasmids encoding PB1, PB2, PA, and NP. Approximately 16 to 18 h posttransfection, the 293T cells were dispersed and cocultured with MDCK-HA cells in DMEM supplemented with 10% FBS. After the cells had formed a monolayer, the medium was replaced with DMEM supplemented with 3.0 μg/ml *N*-acetyl trypsin (NAT; Sigma-Aldrich [Sigma], St. Louis, MO), and virus production was monitored by hemagglutination titer. Virus stocks were propagated in MDCK-HA cells, and the titers were determined by plaque assay on MDCK-HA cells. Mutant and reassortant viruses will be designated by the origin and number of wt gene segments followed by the origin and gene(s) carrying mutations. For example, Ud7+Ud HA-SSS virus contains the wt Ud PB1, PB2, PA, M, NP, NS, and NA genes and the Ud HA gene, with the three conserved cysteines mutated to serines. Viral RNA was extracted from virus stocks using a QIAamp viral RNA kit (QIAGEN, Valencia, CA), transcribed into DNA with AMV Super reverse transcriptase (Molecular Genetic Resources, Tampa, FL), and amplified with AmpliTaq DNA polymerase (Applied Biosystems, Foster City, CA). The complete nucleotide sequences of the HA and M genes were determined using a 3100-Avant genetic analyzer (Applied Biosystems).

Plasmids. The eight genome-sense (pHH21) plasmids and four protein-expressing (pcDNA3.1) plasmids used to generate influenza virus by reverse genetics (Ud and WSN strains) have been described previously (26, 43, 44). The eukaryotic expression plasmid pCAGGS (27) was used to transiently express HA and vesicular stomatitis virus (VSV)-G proteins in BHK, CV1, and HeLa T4 cells. Overlapping PCR was used to introduce site-specific mutations into the HA and M1 genes. 293T cells were transfected using TransIT-LT1 (Mirus, Madison, WI), BHK cells were transfected with Lipofectamine (Invitrogen, Carlsbad, CA), and HeLa T4 cells were transfected using Effectene (QIAGEN), according to the manufacturer protocols.

Analysis of cell-cell fusion. For syncytium formation, BHK cells transiently expressing wt or mutant HA proteins were first treated with 50 μg/ml NAT in phosphate-buffered saline (PBS) for 10 min at 37°C. Cells were then treated for 2 min at 37°C with PBS (pH 4.8) to trigger fusion or PBS (pH 7.0) as a control, followed by incubation in DMEM (pH 7.4) at 37°C for 90 min. Cells were then fixed and stained with Hema 3 solution (Fisher Scientific, Hampton, NH) and photographed using a digital camera (DCS 760; Kodak, Rochester, NY) mounted on an inverted phase-contrast microscope (Diaphot; Nikon Instruments, Melville, NY).

For dye-transfer analysis (35), RBCs were freshly prepared and dual labeled as described (35, 43). RBCs (10% in PBS) were incubated with 15 μl octadecyl rhodamine solution (R18, 10 mg/ml in ethanol; Molecular Probes, Eugene, OR) for 1 h at room temperature and then washed extensively with PBS. R18-labeled RBCs (1% in PBS) were then incubated with 20 μl calcein-AM solution (1 mM in dimethyl sulfoxide; Molecular Probes) for 1 h at 37°C. Dual-labeled RBCs were washed extensively in PBS and resuspended to 1% in PBS.

BHK cells grown on glass coverslips transiently expressing wt or mutant HA proteins were first treated with 50 μg/ml NAT and 0.1 U/ml neuraminidase (*Clostridium perfringens*; Sigma) in PBS for 10 min at 37°C. Cells were then washed with ice-cold PBS and bound with dual-labeled RBCs (0.5 ml of 0.1% RBCs in PBS) for 1 h at 4°C. Cells were washed extensively with ice-cold PBS to remove unbound RBCs. Fusion was triggered by treatment with PBS (pH 4.8 or pH 7.0) as a control for 2 min at 37°C, followed by PBS (pH 7.0) for 10 min at 37°C. Cells were then washed with ice-cold PBS, and the transfer of dyes was observed by using a Zeiss LSM 410 laser-scanning confocal microscope (Carl Zeiss, Thornwood, NY). To analyze the dye transfer between infected cells and dual-labeled RBCs, CV1 cells were infected with virus for 6 h and processed for dye transfer as above.

Virus growth and plaque assay. Confluent MDCK cells were inoculated with virus at a multiplicity of infection (MOI) of 0.001 in DMEM containing 1% bovine serum albumin (BSA) for 1 h at 37°C. Unbound virus was removed by washing with PBS, and the replacement medium was serum-free DMEM

supplemented with 2 μg/ml NAT. At 48 h postinfection (p.i.), the medium was harvested and viral titers were determined by plaque assay on MDCK-HA cells.

For plaque assays, confluent MDCK or MDCK-HA cells in six-well plates were inoculated with appropriate dilutions of virus in DMEM containing 1% BSA for 1 h at 37°C. Unbound virus was removed by washing with PBS. Cells were then overlaid with DMEM-1% agarose supplemented with 1.5 μg/ml NAT and incubated at 37°C for 3 days. Plaques were visualized by immunostaining. Briefly, cells were fixed in 1% glutaraldehyde (Sigma) in PBS for 2 h and then incubated in blocking solution (3% egg albumin [Sigma] in PBS) for 30 min. Cells were incubated with goat anti-Ud serum diluted in blocking solution for 1 h, washed, and then incubated with horseradish peroxidase-conjugated donkey anti-goat immunoglobulin G (IgG) (Jackson Immunoresearch Laboratories, West Grove, PA) secondary antibody diluted in blocking solution for 1 h. Plaques were visualized using an Immuno Pure Metal Enhanced DAB substrate kit (Pierce Biotechnology, Rockford, IL) and photographed.

HA raft association assay. HeLa T4 cells grown on 6-cm dishes were either transiently transfected with wt or mutant HA or infected with virus at an MOI of 1 for 1 h and incubated in DMEM supplemented with 10% FBS. Twelve hours posttransfection or p.i., cells were incubated in DMEM deficient in methionine and cysteine for 30 min, then metabolically labeled with 50 μCi Redivue Promix L-[^{35}S] in vitro cell-labeling mix ([^{35}S] Promix; Amersham Biosciences, Piscataway, NJ) in DMEM deficient in methionine and cysteine for 30 min, followed by a chase incubation in DMEM containing 10% FBS for 2 h at 37°C. Cells were then placed on ice, scraped into ice-cold PBS, pelleted, resuspended in 375 μl Dounce buffer (10 mM HEPES, 10 mM NaCl) containing 0.1 mg/ml soybean trypsin inhibitor (Sigma), 1× protease inhibitor cocktail (Sigma), and 1 mM phenylmethanesulfonyl fluoride (Sigma), and Dounce homogenized on ice.

To evaluate the Triton X-100 (TX-100) solubility of HA, homogenized cells were then extracted with 125 μl of 1% TX-100 (0.25% final TX-100 concentration; Sigma) in NTE (100 mM NaCl, 10 mM Tris [pH 7.4], 1 mM EDTA) for 15 min on ice. The samples were then centrifuged at 14,000 × *g* for 30 min at 4°C in a tabletop centrifuge. Supernatant containing the soluble fraction was adjusted to 1× RIPA buffer (1% deoxycholic acid, 1% TX-100, 0.1% sodium dodecyl sulfate [SDS], 10 mM Tris [pH 7.4]) plus 0.15 M NaCl prior to immunoprecipitation. The pellet containing TX-100 insoluble material was resuspended in 1× RIPA plus 0.15 M NaCl buffer and sonicated for ~20 s prior to immunoprecipitation.

Antibodies, immunoprecipitation, and SDS-PAGE. Goat serum raised to purified Ud virus (goat anti-Ud) was used to detect HA, NP, and M1 by immunoprecipitation or immunoblotting. Monoclonal mouse anti-VSV-G antibody (clone P5D4; Sigma) was used to immunoprecipitate VSV-G protein, which was used as a control for a TX-100 soluble, nonraft-associated protein (36).

For immunoprecipitation, appropriate antibody was added to samples adjusted to 1× RIPA plus 0.15 M NaCl buffer and incubated for 1 h at 4°C. Immune complexes were precipitated by incubation with a protein A/G Sepharose 3:1 mixture (Amersham Biosciences) for 30 min at 4°C. Sepharose beads were washed three times with 1× RIPA plus 0.3 M NaCl, once with 1× RIPA plus 0.15 M NaCl, and once with SDS wash II buffer (150 mM NaCl, 50 mM Tris [pH 7.4], 2.5 mM EDTA). Samples were resuspended in SDS loading buffer (50 mM Tris [pH 6.8], 100 mM dithiothreitol, 2% SDS, 0.1% bromophenol blue, 10% glycerol) and boiled for 5 min, and polypeptides were fractionated by SDS-PAGE (polyacrylamide gel electrophoresis) on a 15% polyacrylamide gel. Quantification of radioactivity was performed with a Fuji BioImager 1000 and Image Gauge version 3.3 software (Fuji Medical Systems, Stanford, CT).

Virus release assay and immunoblotting. Confluent MDCK cells grown in 6-cm dishes were inoculated with virus at an MOI of 1 in DMEM-1% BSA for 1 h at 37°C. The inoculum was removed and replaced with DMEM supplemented with 10% FBS and 0.1 mg/ml soybean trypsin inhibitor to prevent multiple rounds of infection. Twenty hours p.i., the culture medium was harvested and cellular debris were removed by centrifugation. The medium was then layered onto a 20% sucrose-NTE (wt/vol) cushion and ultracentrifuged at 200,000 × *g* for 2 h at 4°C in a Beckman Ti70.1 rotor using a Beckman Optima XL-80 ultracentrifuge (Beckman Coulter, Fullerton, CA). The pellet was resuspended in 0.5 ml NTE and homogenized by passage through a 23 G needle. The suspension was mixed with 1.3 ml 80% sucrose-NTE (wt/vol) and then overlaid with 1.8 ml 50% sucrose-NTE (wt/vol), followed by 0.6 ml 10% sucrose-NTE (wt/vol). Samples were ultracentrifuged at 200,000 × *g* for 18 h at 4°C in a Beckman Ti70.1 rotor. The top fraction (2.1 ml) was harvested, diluted in NTE, and ultracentrifuged at 200,000 × *g* for 2 h. Finally, the pellet was resuspended in SDS loading buffer, boiled for 5 min, and analyzed by SDS-PAGE on a 15% polyacrylamide gel. For the cellular fraction, infected cells were lysed in SDS loading buffer, sonicated for ~20 s, and boiled for 5 min and proteins were resolved by SDS-PAGE on a 15% polyacrylamide gel.

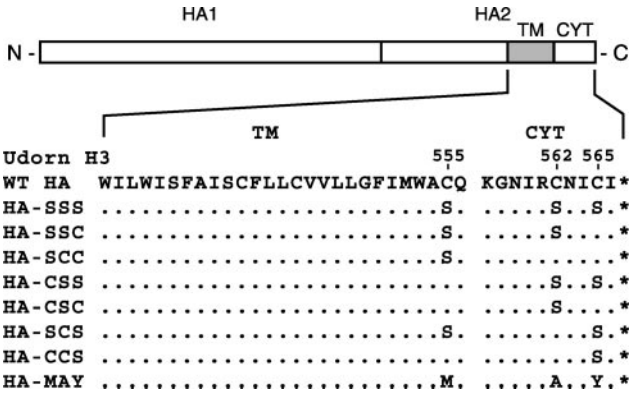

FIG. 1. Influenza virus Ud HA (H3) palmitoylation site mutants. The amino acid sequences of Ud HA in the region of the TM domain and cytoplasmic tail (CYT) are shown. The conserved cysteine residues are at positions 555, 562, and 565. The cysteine substitution mutants and their nomenclature are shown. Amino acid residues that are the same as that of the wild type are indicated by •, and * indicates the HA stop codon.

To detect viral proteins by immunoblotting, proteins were transferred to polyvinylidene difluoride membranes (Millipore, Billerica, MA) using standard procedures. Membranes were blocked in Odyssey blocking buffer (Li-Cor Biosciences, Lincoln, NE) and then incubated with goat anti-Ud serum in blocking buffer with 0.1% Tween 20 (Sigma) for 1 h, followed by incubation with Alexa Fluor 680-conjugated donkey anti-goat IgG (Molecular Probes) secondary antibody in blocking buffer with 0.1% Tween 20 for 1 h. Proteins were detected and quantified with an Odyssey infrared imaging system (Li-Cor Biosciences).

RESULTS

Generation of mutations in the C-terminal conserved cysteines of influenza virus HA. To examine the role of palmitoylation of the three conserved cysteines in the C-terminal transmembrane-cytoplasmic tail region of influenza virus HA, cysteine-to-serine mutations were introduced into the Ud HA (H3 subtype) gene at residues 555, 562, and 565, in all possible combinations (Fig. 1). It had been established previously that the presence of the cysteine residue per se was not required for HA function (15, 42). Herein, the HA cysteine mutants will be designated by the residue (cysteine or serine) found at each position in residue order, e.g., mutation of all three cysteine residues is abbreviated to Ud HA-SSS. An additional HA mutant in which the three cysteines in order were mutated to methionine, alanine, and tyrosine (Ud HA-MAY) was also generated. This HA mutant had been shown previously to be nonpalmitoylated and could be recovered in a WSN genetic backbone (WSN7+Ud HA-MAY) (15). Palmitoylation site HA mutants were then analyzed, either by expression from cDNA by transient transfection or by use of the mutants to recover mutant Ud viruses by using a highly efficient reverse genetics system (26). To facilitate recovery of greatly debilitated viruses, 293T cells initially transfected with eight genome-encoding plasmids and four protein (PB1, PB2, PA, and NP)-expressing plasmids were cocultured with MDCK-HA cells, a *trans*-complementing wt Ud HA-expressing MDCK cell line (43). By using this system, all HA palmitoylation site mutant viruses were recovered, although, in most cases, mutants were recovered less efficiently than wt virus (data not shown). Influenza viruses produced using

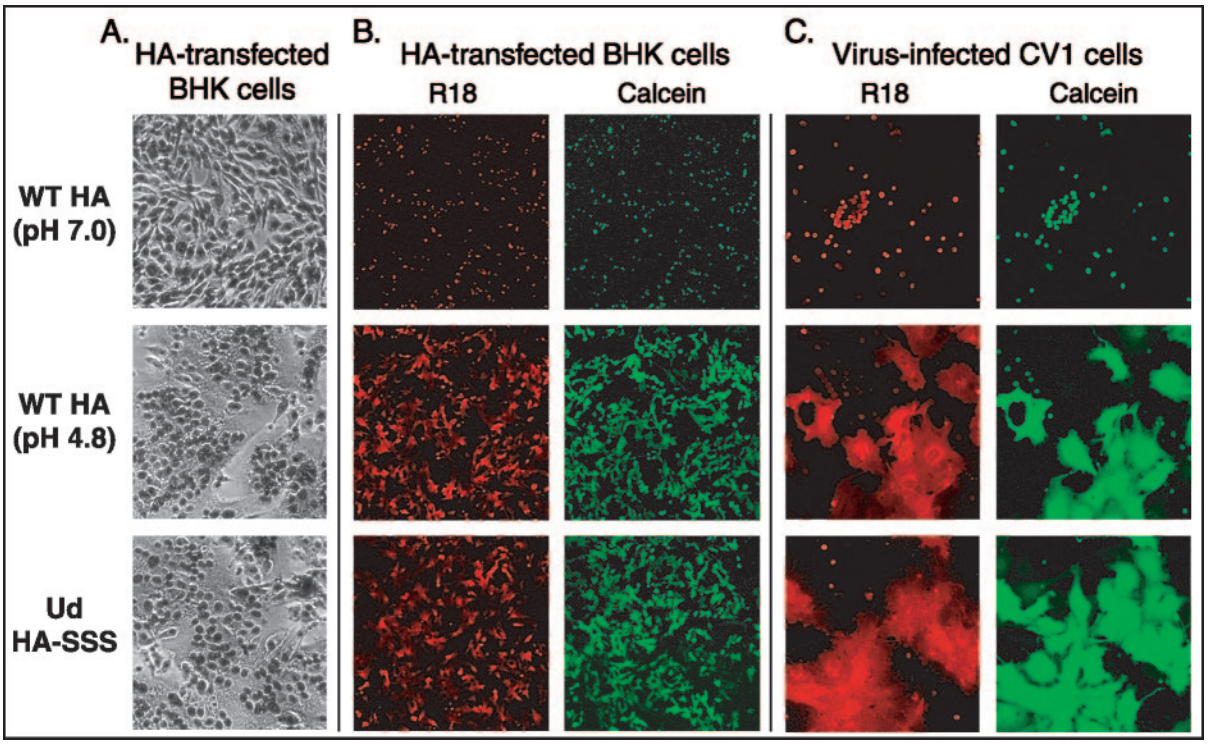

FIG. 2. Analysis of wt Ud HA and Ud HA-SSS in cell-cell fusion. (A) Syncytium formation between BHK cells transfected with wt HA or Ud HA-SSS. Cells were treated with trypsin to cleave HA and were either mock treated with PBS pH 7.0 or triggered for fusion with PBS pH 4.8 for 2 min, and then the medium was replaced with DMEM pH 7.4. After 90 min of incubation, cells were fixed, stained, and photographed. (B and C) Dye transfer between R18 (red)/calcein (green) dual-labeled RBCs and transfected BHK cells (B, magnification, 10×) or wt Ud virus or Ud7+Ud HA-SSS virus-infected CV1 cells (C, magnification, 40×). As described in Materials and Methods, cells were trypsin and neuraminidase treated prior to mock treatment with PBS pH 7.0 or fusion being triggered with PBS pH 4.8.

this system are pseudotyped with wt Ud HA but contain a mutated Ud HA gene.

Lack of HA palmitoylation does not affect HA-mediated fusion. The capacity of the HA mutants to cause low pH-induced syncytium formation in HA-transfected BHK cells was examined (Fig. 2A). All the mutant HA proteins showed comparable surface expression as determined by flow cytometry (data not shown). Compared to mock-treated cells, wt Ud HA-transfected cells treated at pH 4.8 for 2 min and incubated for a further 90 min in neutral pH DMEM were nearly completely fused with giant syncytia throughout the dish. Extensive syncytium formation was also observed for mutant Ud HA-SSS (Fig. 2A). All other possible combinations of the cysteine-mutated HA proteins also showed syncytium formation (data not shown).

Consistent with the syncytium formation data, dye transfer between R18/calcein dual-labeled RBCs and HA-transfected BHK cells was also unaffected by the mutation of the conserved cysteine residues in all possible combinations. Only data for Ud HA-SSS are shown (Fig. 2B). After a mock neutral pH treatment, only unfused dual-labeled RBCs were observed. However, treatment with buffer at pH 4.8 caused lipid mixing and cytoplasmic content mixing between RBCs and HA-transfected BHK cells, as observed by the spreading of the red lipidic dye R18 and spreading of the green cytoplasmic dye calcein. For all HA cysteine-mutated proteins, the dye transfer of both R18 and calcein was coincident in all cases.

To test whether there was a requirement for HA palmitoylation for fusion in the context of a virus infection, the dye transfer (R18 and calcein) between RBCs and influenza virus-infected cells was also examined. CV1 cells were infected with wt Ud virus or Ud containing Ud HA-SSS (Ud7+Ud HA-SSS). In both cases, lipid dye transfer and cytoplasmic dye transfer were observed (Fig. 2C), indicating that, for H3 HA, palmitoylation was not required in the context of a viral infection for HA-mediated fusion.

HA palmitoylation is required for efficient virus replication. When Ud viruses containing HA palmitoylation site mutants (Ud7+Ud HA mutants) were rescued and examined for plaque phenotype (Fig. 3) and virus growth (Fig. 4), dramatic differences were observed depending on both the position of the mutant cysteine residue and the number of cysteine residues retained. All of the mutant viruses were able to form plaques on the MDCK-HA cell line as expected due to complementation with wt HA. However on regular MDCK cells, no plaques were observed when all three cysteines were mutated to serine in the Ud7+Ud HA-SSS virus (Fig. 3). The ability to form small plaques was restored with the Ud7+Ud HA-SSC mutant. The Ud7+HA-SCC mutant produced a plaque phenotype similar to wt virus. However, for the Ud7+Ud HA-CSS mutant, no virus plaques were observed.

The replication of the HA cysteine-mutant viruses was tested by infecting cells at a low MOI (0.001) and measuring the titer of virus produced at 48 h p.i. Consistent with the

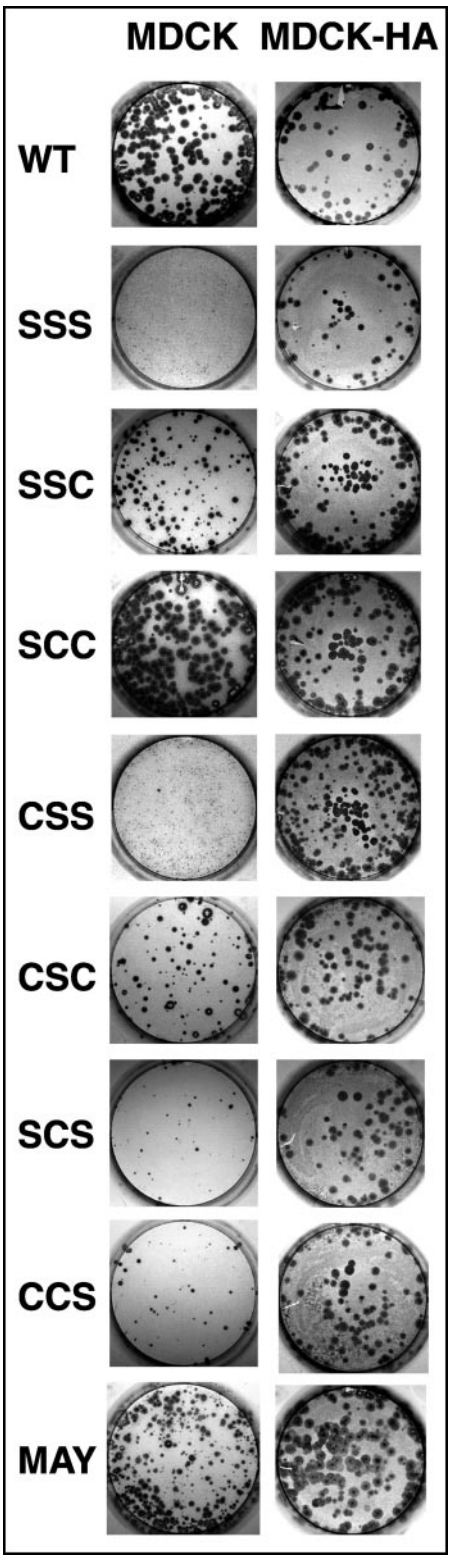

FIG. 3. Plaque phenotypes of HA palmitoylation mutant viruses. Ud influenza virus and derivatives containing mutations of the conserved HA cysteine residues were recovered from cDNA and assayed for plaque formation on MDCK and MDCK-HA cells. After 3 days of incubation, plaques were immunostained using goat anti-Ud serum, followed by horseradish peroxidase-conjugated secondary antibody and metal-enhanced DAB substrate. All viruses are Ud7+Ud HA or Ud7+Ud HA mutant.

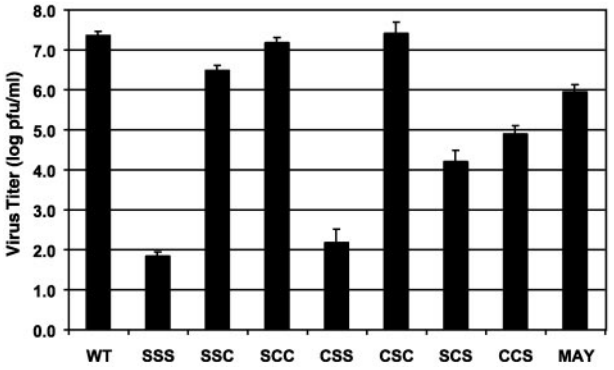

FIG. 4. Growth titers of HA palmitoylation mutant viruses. MDCK cells were infected at an MOI of 0.001. At 48 h p.i., the culture supernatant was harvested and the virus titer was determined by plaque assay on MDCK-HA cells. Error bars represent standard deviations from the average of three experiments. All viruses are Ud7+Ud HA or Ud7+Ud HA mutant.

plaque phenotype data, all viruses grew efficiently in the MDCK-HA cell line (data not shown). In regular MDCK cells, however, both the Ud7+Ud HA-SSS and Ud7+Ud HA-CSS mutant viruses had titers of $\sim 1 \times 10^2$ PFU/ml, a 5-log decrease in maximal titer compared to that of wt Ud virus (Fig. 4). Mutants Ud7+Ud HA-SCS and Ud7+Ud HA-CCS exhibited improved replication ($\sim 1 \times 10^4$ PFU/ml and $\sim 1 \times 10^5$ PFU/ml), and mutants Ud7+Ud HA-SSC, Ud7+Ud HA-SCC, and Ud7+Ud HA-CSC showed titers of approximately the level of that of the wt Ud virus ($\sim 1 \times 10^7$ PFU/ml). These data suggest that the third palmitoylation site (on cysteine residue 565) has the greatest influence on virus replication, with a contribution from the second site (cysteine residue 565). However, palmitoylation at the first cysteine residue (555) does not appear to be important for virus replication.

In our previous study (15), when the MAY mutation was introduced into the Ud HA gene and recovered in the WSN genetic background (WSN7+Ud HA-MAY), the mutant virus was replication competent with only an ~1.5-log decrease in replication, despite having all three palmitoylation sites ablated (15). Using our homotypic Ud genetic backbone system, it was also found that the Ud7+Ud HA-MAY virus was replication competent but with an ~1.5-log decrease in replication (Fig. 4), and the Ud7+Ud HA-MAY virus was able to form plaques on MDCK cells (Fig. 3).

Lipid raft association is affected by the removal of palmitoylation sites but does not correlate with virus replication. As HA TM domain mutants that diminish HA raft association were shown previously to decrease efficient virus replication (43), it seemed possible that the removal of HA palmitoylation sites would decrease raft association and hence explain the decrease in virus replication efficiency in the context of the homotypic Ud genetic backbone. Raft association of the HA cysteine mutants was tested by performing 0.25% TX-100 extraction at 4°C using both cells transiently expressing HA and mutant virus-infected cells. In HeLa T4 cells transfected with mutant HAs (Fig. 5A and C), ~65% of wt HA was resistant to TX-100 extraction, whereas nonraft-associated VSV-G (36) was only ~5% insoluble. For both Ud HA-SSS and Ud HA-MAY mutants expressed in HeLa T4 cells, HA insolubility

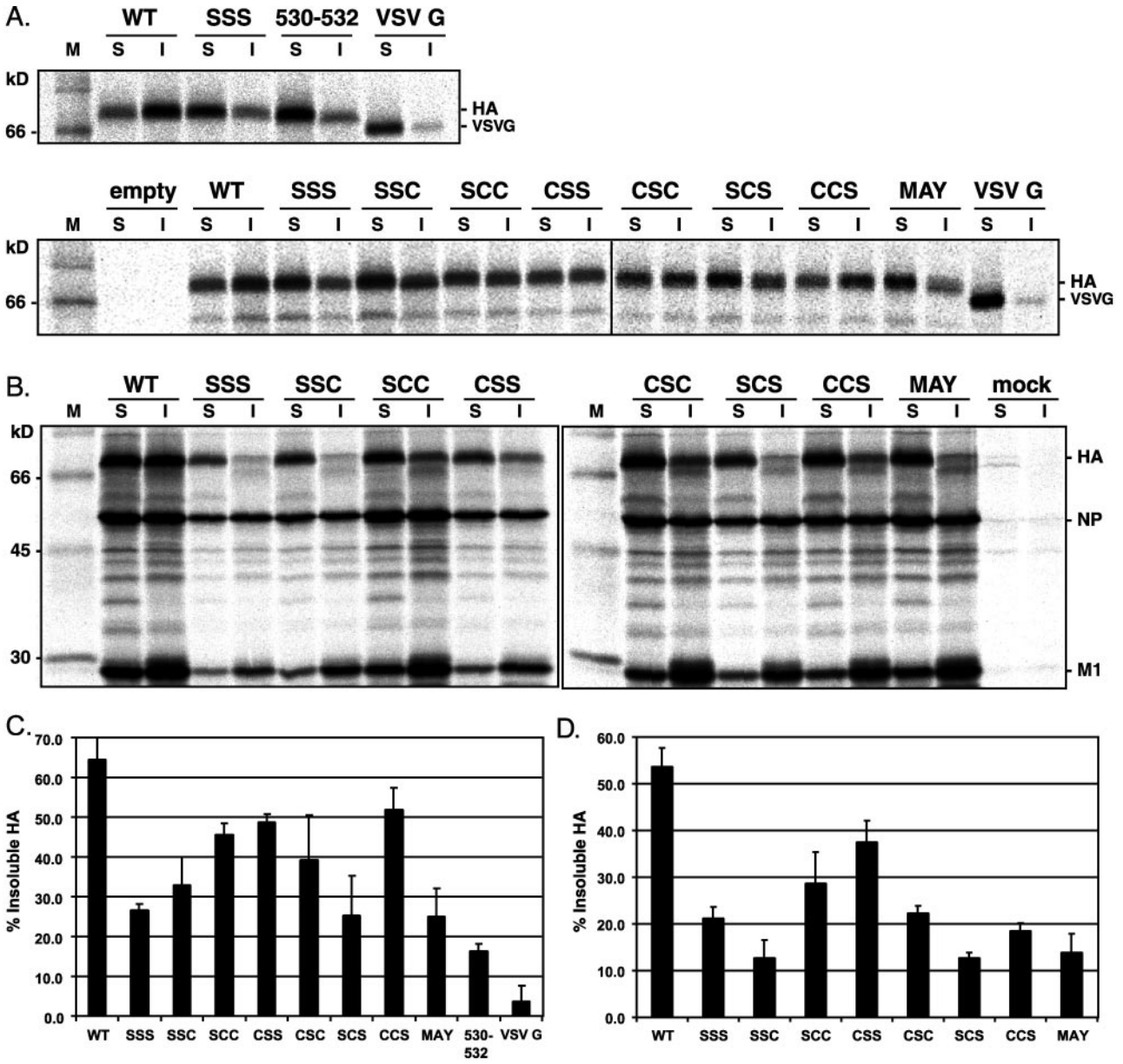

FIG. 5. TX-100 insolubility of palmitoylation site mutated HA. (A) HeLa T4 cells transfected with wt or mutated Ud HA or empty pCAGGS vector were pulse labeled with [^{35}S] Promix and extracted in 0.25% TX-100 at 4°C. Soluble (S) and insoluble (I) fractions were separated by centrifugation and immunoprecipitated with goat anti-Ud serum, and polypeptides were analyzed by SDS-PAGE. Nonraft HA TM mutant 530-532 has been described previously (43) and is used here as a control. VSV-G protein was included as a control for a TX-100 soluble, nonraft-associated protein (36) and was immunoprecipitated with a mouse anti-VSV-G antibody. M, ^{14}C-labeled methylprotein molecular mass marker (Amersham Biosciences). (B) HeLa T4 cells were infected with wt or Ud7+Ud HA mutant virus at an MOI of 1 for 12 h or mock infected, and then TX-100 insolubility of HA was analyzed as above. M, ^{14}C-labeled methyl protein molecular mass marker (Amersham Biosciences). (C and D) The percent total HA radioactivity found in the insoluble fraction in transfected (C) or virus-infected (D) cells was quantified using Image Gauge. Error bars represent the standard deviation from the average of three experiments.

decreased to ~25%. As a comparison, we analyzed the previously studied HA TM mutant 530-532 (43) and it was found to have a TX-100 insolubility that was consistently lower (~15%) than that of any of the HA palmitoylation mutants. We suggest the drastic effect of HA TM mutant 530-532 on raft association is because its TX-100 insolubility is below the minimum threshold value needed for raft association. HA mutants containing the second or third cysteine residues alone (Ud HA-SSC or Ud HA-SCS) did not exhibit significantly greater HA insolubility compared to that of Ud HA-SSS. However, cDNA-expressed Ud HA-SCC, Ud HA-CSS, and Ud HA-CCS mutants were largely insoluble in TX-100 (~50%), indicating a greater degree of raft association compared to that of the expressed Ud HA-SSS mutant.

In influenza virus-infected HeLa T4 cells (Fig. 5B and D) and MDCK cells (data not shown), HA insolubility followed a

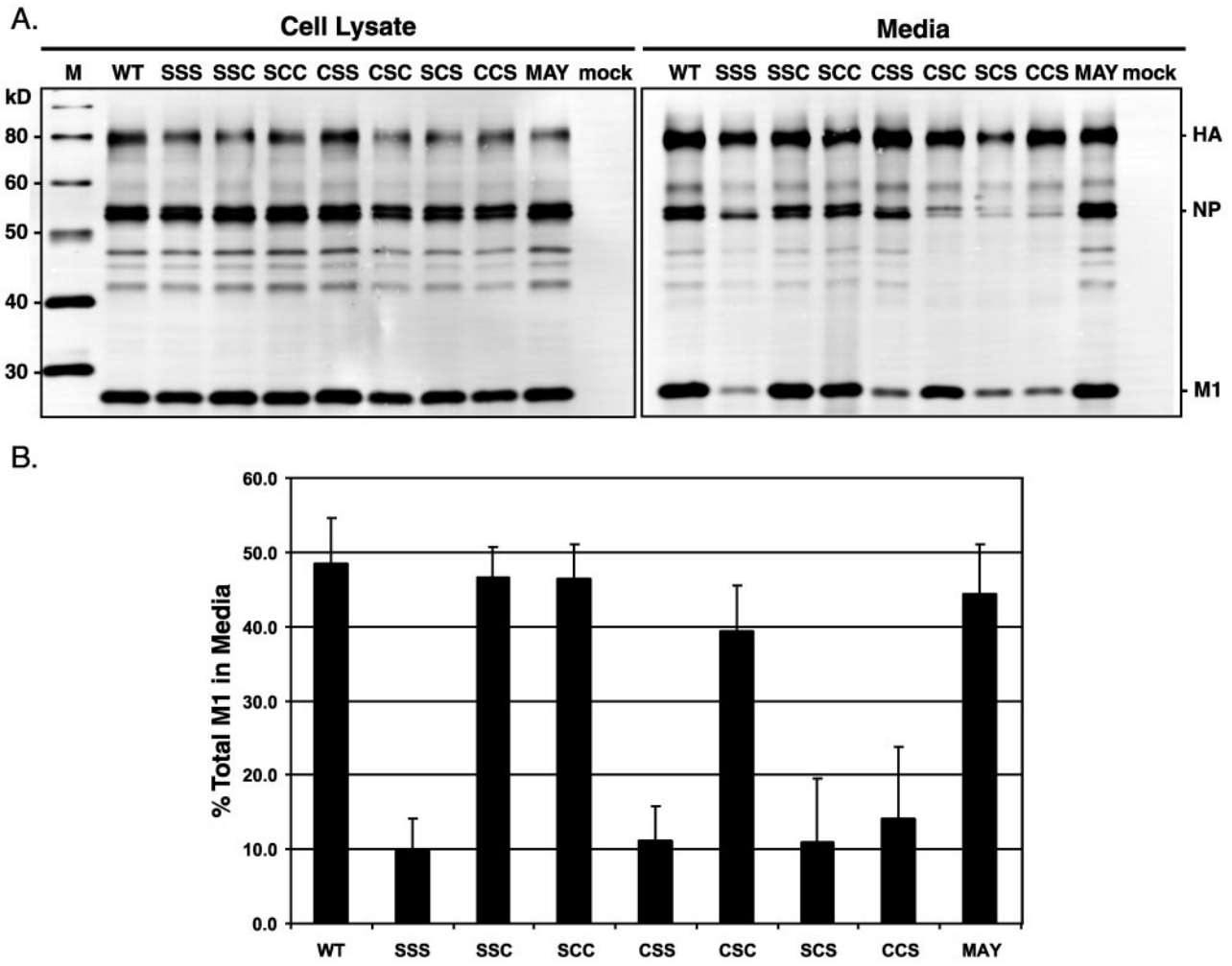

FIG. 6. Assembly and release of HA palmitoylation site mutant viruses. (A) MDCK cells were infected with wt or Ud7+Ud HA mutant virus at an MOI of 1, or mock infected, and incubated in DMEM with 10% FBS and soybean trypsin inhibitor for 20 h. The culture medium was harvested, and virions were purified through a 20% sucrose cushion, followed by flotation through a discontinuous sucrose gradient. Purified virions were pelleted by centrifugation and resuspended in SDS loading buffer, and polypeptides were analyzed by SDS-PAGE. To analyze the virus-specific proteins synthesized in virus-infected cells, the cells were lysed in SDS loading buffer and sonicated and polypeptides were subjugated to SDS-PAGE. Polypeptides were detected by immunoblotting with goat anti-Ud serum, followed by Alexa Fluor 680-conjugated donkey anti-goat secondary antibody, and visualized using an Odyssey infrared imaging system. NP appears as a doublet which probably reflects the known proteolytic clip of NP (52). M, MagicMark western protein standard (Invitrogen). (B) The percentage of total M1 found in the medium fraction was quantified using the Odyssey imaging software. Error bars represent standard deviations from the average of three experiments.

related trend, with some differences from that found in cells transiently expressing HA. However, the striking result was that Ud7+Ud HA-SCC and Ud7+Ud HA-CSS, viruses that exhibited an ~5-log difference in infectivities, had HAs that showed fairly similar TX-100 insolubilities (~30 to 40%). These data indicate a lack of a direct correlation between HA raft association, palmitoylation, and virus growth. Some mutant HAs showed a difference in TX-100 insolubility, depending on whether the HA was expressed from cDNA or in virus-infected cells. This may reflect the association of viral proteins with the HA cytoplasmic tail in virus-infected cells (see below).

Removal of HA palmitoylation sites affects virus assembly. To assess the efficiency of the mutant HA viruses to assemble, MDCK cells were infected with virus at an MOI of 1 under single-round infection conditions. Immunoblotting of infected cell lysates showed that expressions of viral proteins were approximately equivalent (Fig. 6A). The protein composition of virus particles released into the medium was analyzed by SDS-PAGE and immunoblotting. When normalized to M1 found in the cell lysate, ~50% of total M1 was found released into the medium following wt Ud virus infection (Fig. 6A and B). However, for Ud7+Ud HA-SSS, Ud7+Ud HA-CSS, Ud7+Ud HA-SCS, and Ud7+Ud HA-CCS, the amount of total M1 found in the medium was reduced significantly to ~10%. Concomitantly, there was a decrease in the amount of NP protein released into the medium. These viruses also exhibited 2- to 5-log decreases in infectivity compared to that of wt virus (Fig. 4). In contrast, those viruses that contained a cysteine at residue 565 (Ud7+Ud HA-SSC, Ud7+Ud HA-SCC, and Ud7+Ud HA-CSC) released amounts of M1 and NP into the

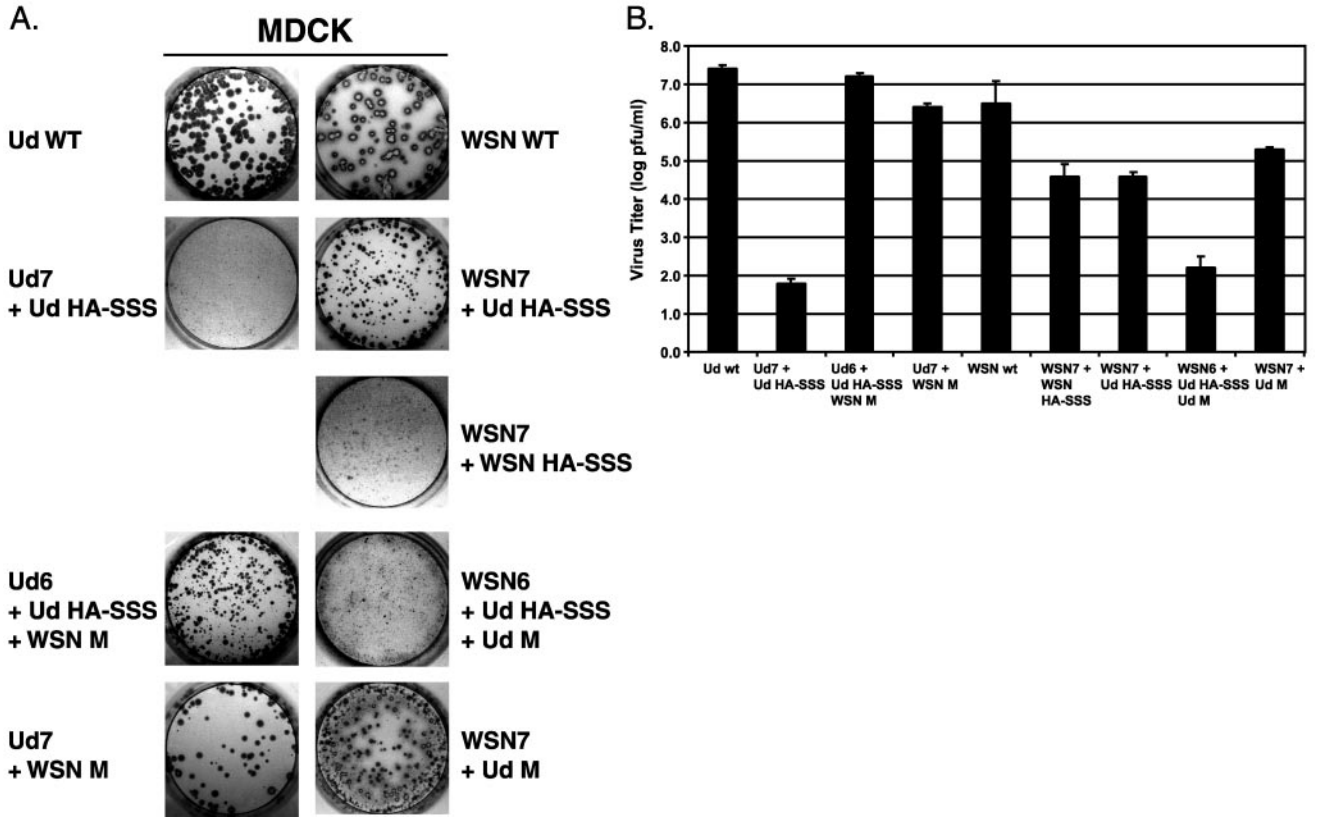

FIG. 7. Plaque phenotypes and titers of Ud and WSN reassortant viruses. (A) Wt and mutant Ud and WSN reassortant viruses were recovered in MDCK-HA cells and plaque assayed on MDCK cells. Ud7+Ud HA-SSS virus did not form plaques, whereas WSN7+Ud HA-SSS was able to form plaques. WSN7+WSN HA-SSS formed poorly staining but distinct plaques. Plaque-forming ability was observed for Ud6+Ud HA-SSS+WSN M, but WSN6+Ud HA-SSS+Ud M virus produced only pinpoint plaques. Both Ud and WSN virus bearing the heterologous M gene were able to form plaques. (B) Growth titers of viruses were determined as described in the legend to Fig. 4.

media similar to that of wt virus and these viruses had wt infectivity (Fig. 4). Ud7+Ud HA-MAY virus was released efficiently, despite the lack of palmitoylation sites; however, this is not surprising given the fact that this virus was able to replicate efficiently in MDCK cells. The data suggest a unique property of the MAY mutation, and given that M555 is found in some naturally occurring HA isolates (H8 and H9 subtypes), the replication competency of Ud7+Ud HA-MAY is most likely due to the bulky hydrophobic tyrosine residue (Y565).

Replication of WSN virus-containing Ud HA-SSS. Many earlier studies to investigate the role of HA palmitoylation in the influenza virus life cycle used as the genetic backbone the high-yielding mouse-adapted WSN strain of influenza virus (15, 51, 53). The original influenza virus reverse genetics system (20) was used in these studies, and viruses were not recovered when cysteine 565 was substituted (15, 53), but the H3 HA-MAY mutant could be recovered in the WSN genetic background (15). As the Ud HA-SSS mutation has a profound effect on growth in the Ud genetic background (Fig. 3 and 4), we determined the effect of Ud HA-SSS on growth in the WSN genetic backbone by using the newer higher efficiency rescue system (26). The WSN7+Ud HA-SSS virus formed plaques in MDCK cells (Fig. 7A), and the virus grew to a titer ($\sim 5 \times 10^4$ PFU/ml) only 2 logs less than that of wt WSN. Another virus, WSN7+WSN HA-SSS (H1 subtype), also had a titer 2 logs lower than that of wt WSN and formed plaques on MDCK cells that stained poorly but formed distinctly in contrast to the plaque phenotype of Ud7+Ud HA-SSS.

The WSN M gene restores replication of Ud virus-containing Ud HA-SSS. As the Ud HA-SSS mutation in the Ud genetic backbone caused decreased virus assembly, we rationalized that the decrease in virus titers for virions containing HA that lack palmitoylation may be linked to the M1 protein and that differences between WSN and Ud M1 proteins would contribute to the observed differing dependence on H3 HA palmitoylation. To test whether the origin of the M gene encoding M1 and M2 proteins was important for the growth differences between Ud containing Ud HA-SSS and WSN containing Ud HA-SSS, the M gene was swapped between the viruses (Ud6+Ud HA-SSS+WSN M and WSN6+Ud HA-SSS+Ud M). As shown in Fig. 7A and B, Ud6+Ud HA-SSS+WSN M virus formed plaques in MDCK cells and had a titer ($\sim 1 \times 10^7$ PFU/ml) equivalent to that of the wt Ud virus, unlike Ud7+Ud HA-SSS which failed to produce plaques and had a titer of $\sim 1 \times 10^2$ PFU/ml. In the reciprocal experiment, WSN6+Ud HA-SSS+Ud M formed only pinpoint plaques and had a titer of $\sim 1 \times 10^2$ PFU/ml (Fig. 7A and B), unlike WSN7+Ud HA-SSS, which formed plaques and had a titer of $\sim 5 \times 10^4$ PFU/ml. The origin of the M gene itself did not cause these phenotypes, as Ud7+WSN M and WSN7+ Ud M

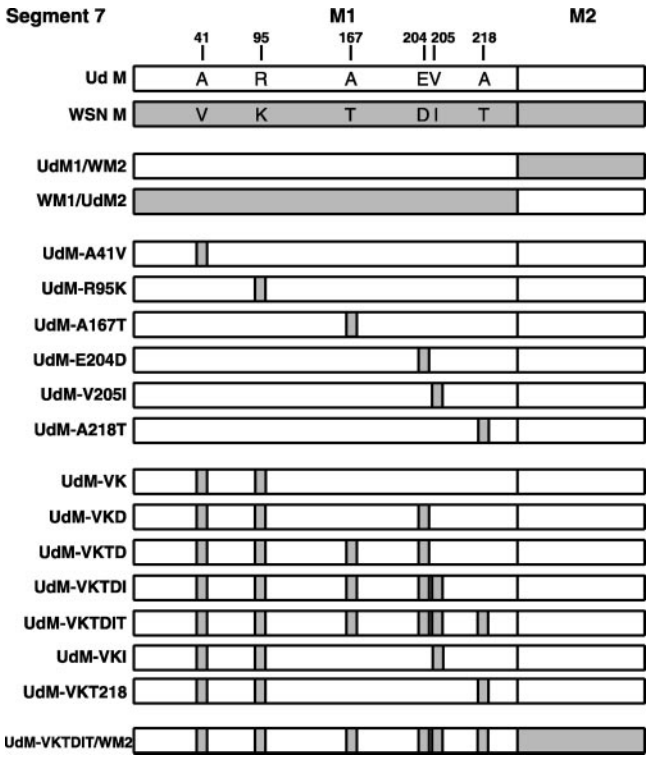

FIG. 8. Schematic diagram showing the amino acid differences between Ud and WSN M1 protein sequences and chimeric M mutants tested in this study. Ud (GenBank accession no. J02167) and WSN (GenBank accession no. L25818) M1 proteins differ at six residues as shown. Differences in the M2 sequence are not shown for simplicity. Ud viruses with nonpalmitoylated HA containing M1/M2 of either Ud or WSN were generated (Ud6+Ud HA-SSS+UdM1/WM2 and Ud6+Ud HA-SSS+WM1/UdM2). Ud viruses with nonpalmitoylated HA containing substitutions, either singly or in various combinations, of the six differing residues between Ud and WSN M1 were also generated (Ud6+Ud HA-SSS+mutated UdM). The corresponding WSN M1 residues in Ud M1 are shown by the gray box.

viruses both formed plaques and had good growth titers (Fig. 7A and B).

The WSN M1 protein alone restores growth to Ud7+Ud HA-SSS. Influenza virus RNA segment 7 (the M gene) encodes two proteins, M1 and M2 (17). To determine which of these two proteins conferred the growth differences to Ud7+Ud HA-SSS, chimeric M genes were constructed between Ud and WSN (UdM1/WM2 and WM1/UdM2) such that the encoded amino acids precisely reflected their parental amino acid sequences (Fig. 8). These chimeric M genes were introduced into Ud7+Ud HA-SSS to yield Ud6+Ud HA-SSS+UdM1/WM2 and Ud6+Ud HA-SSS+WM1/UdM2. Replication of Ud6+Ud HA-SSS+UdM1/WM2 in MDCK cells was ~1 log better than Ud7+Ud HA-SSS, whereas Ud6+Ud HA-SSS+WM1/UdM2 grew to a titer almost like that of the wt Ud virus (Fig. 9). These data indicate that the WSN M1 protein is responsible for rescuing replication of the palmitoylation-deficient Ud HA-SSS in the Ud6 genetic backbone.

The Ud and WSN M1 proteins differ at only six amino acids (Fig. 8). Several of these six residues have been implicated in defining virus morphology as spherical or filamentous (5, 8, 31, 47, 49), affecting vRNP binding (19), and affecting the ability of the 14C2 M2-specific monoclonal antibody to restrict the growth of Ud virus (49). Single residue mutations were made, changing Ud M1 residues to their corresponding WSN M1 residues, and it was found that no one residue appeared to fully restore replication of Ud6+Ud HA-SSS+mutated UdM (Fig. 9). As the M1 mutations A41V and R95K have both been implicated in converting Ud virus from filamentous to spherical morphology (5, 8, 31), it seemed possible that, together, these residues may influence virus replication. When the mutations were made in combination, virus replication increased significantly, yielding a titer ~1.5 log units lower than that of the wt Ud virus (Fig. 9). Additional combinations of mutated M residues were constructed as shown (Fig. 8), although only virus with the Ud M1 protein containing all six WSN M1 mutations (Ud6+Ud HA-SSS+UdM-VKTDIT) fully restored replication of Ud7+Ud HA-SSS to wt levels (Fig. 9). Thus, these data indicate there is an incompatibility between the Ud M1 and nonpalmitoylated Ud HA that can be overcome by the constellation of six differing residues in the WSN M1 protein.

DISCUSSION

The C terminus of the influenza virus HA protein contains three cysteine residues that are highly conserved among HA subtypes. By using a highly efficient reverse genetics recovery system and a *trans*-complementing MDCK-HA cell line, we were able to recover mutant Ud viruses containing the HA gene encoding cysteine-to-serine substitutions of all three conserved cysteine residues and in all possible combinations. However, Ud7+Ud HA-SSS showed a 5-log decrease in titer compared to that of the wt virus.

Previous studies on the role of HA palmitoylation in the influenza virus life cycle had led to differing data, depending on the HA subtype studied. For the H3 HA subtype, the data have shown consistently that palmitoylation of HA is not required for fusion activity (15, 21, 41, 42) and here we have extended that conclusion by showing that nonpalmitoylated H3 HA is active in both the lipid-mixing and content-mixing steps of fusion for both HA expressed from cDNA and HA expressed in the context of a virus infection. However, for other subtypes, including H1, H2, and H7, the fusion activity of nonpalmitoylated HA varied among reports, even for a given subtype, ranging from full activity to impairment or inactivity (10, 23, 24, 30, 34, 45, 46). Perhaps at greatest odds are differences between the H3 and H7 HA subtypes. Initially, palmitoylation of vector-expressed H7 HA was not thought to be required for fusion (30, 45), although a subsequent study (10) found that when nonpalmitoylated H7 HA was protected by coexpression of M2, syncytium formation, but not dye transfer, was reduced. Recently, in the context of recovered A/FPV/Rostock/34 virus, H7 HA mutants lacking palmitoylation at the second or third cysteines were unable to facilitate complete pore formation in dye-transfer experiments (46). In our study, we observe no difference in the ability of nonpalmitoylated H3 HA to induce fusion whether expressed alone or in the context of virus. One possible explanation for the discrepancy in the palmitoylation requirement for fusion between HA subtypes is that HA palmitoylation may influence the kinetics of fusion differently among subtypes. One study demonstrated that nonpalmitoy-

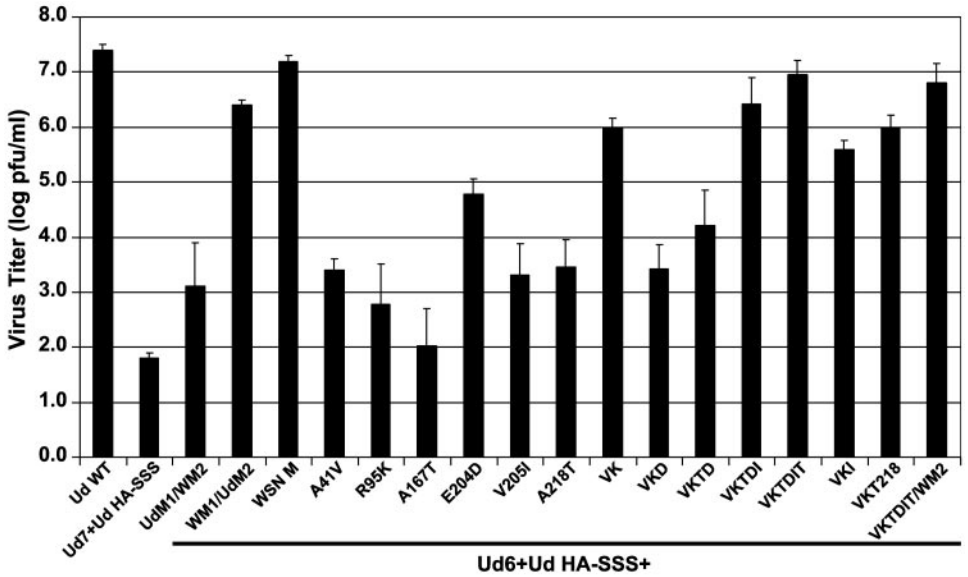

FIG. 9. Growth titers of the Ud6+Ud HA-SSS viruses that contained mutant M1 proteins determined as described in the legend to Fig. 4.

lated H3 HA reduced the amount of "pore flickering" observed prior to full fusion, although no difference in pore formation was found overall (21). This may indicate that the role of HA palmitoylation in fusion is subtle and may vary between HA subtypes and that present fusion studies are not sufficiently quantitative to be compared between reports. Much as it would be useful to compare HA subtypes in one laboratory, we cannot perform studies in our laboratory with either H2N2 or A/FPV/Rostock/34 virus, as we lack a CDC/NIH/USDA-mandated BSL3+ containment facility.

We considered it possible that the growth defect of Ud7+Ud HA-SSS could be due to a failure of Ud HA-SSS to concentrate in lipid raft microdomains, particularly as influenza virus buds from lipid rafts (36) and mutations in the HA TM domain affect HA raft association and budding of virus (43). Furthermore, palmitoylation of some cellular integral membrane proteins (e.g., LAT [11], CD81 [7], and Src family tyrosine kinases [16]) has been shown to be required for lipid raft association. Our analysis of the TX-100 insolubility at 4°C of the HA palmitoylation mutants indicated that many of the mutant HA proteins had reduced insolubility in TX-100. However, the change in insolubility was not as profound as observed with the HA TM domain mutations that affect HA concentration at the plasma membrane and result in decreased virus budding (43). For expressed HA, HA mutants containing the first cysteine residue (C555), either alone (Ud HA-CSS) or with other cysteines present (Ud HA-CSC and Ud HA-CCS) appeared to have the greatest degree of HA raft association. This may be due to the position of C555 in the TM domain, where it may be important for the association of HA with rafts. However, the addition of cysteine residues (from Ud HA-CSS to Ud HA-CSC or Ud HA-CCS) did not appear to increase HA raft association in an additive manner, suggesting that palmitoylation at C562 and C565 may not be primarily important for HA raft association. In the context of virus infection where other viral proteins were expressed, removal of palmitoylation sites appeared to weaken HA raft association, leading to more transient raft association as observed for HAs of Ud7+Ud HA mutant viruses. Importantly, we found there was no direct correlation between the change in HA TX-100 insolubility and virus assembly for the HA palmitoylation mutants. Thus, although palmitoylation of HA affects HA raft association, this does not appear to be the primary function of palmitoylation and does not explain the 5-log reduction in titer of Ud7+Ud HA-SSS compared to that of the wt Ud virus. Palmitoylation may be an additional or redundant feature of HA that works with the TM domain in promoting association of HA with lipid rafts.

When the polypeptide composition of the HA palmitoylation site mutant virus released into the media was examined, it was found that there was a correlation between reduced virus particle release and lack of palmitoylation at residue 565. The Ud7+Ud HA-SSS and Ud7+Ud HA-CSS viruses, which had 5-log drops in infectivity compared to that of the wt Ud virus, and Ud7+Ud HA-SCS and Ud7+Ud HA-CCS, which had 2- to 3-log drops in infectivity compared to that of the wt Ud virus, all showed greatly reduced amounts of M1 and NP proteins in the released virus-like particles, suggesting that palmitoylation of the cysteine residue 565 is very important for assembly of the Ud virus particle. Palmitoylation of the penultimate cysteine (residue 562) may compensate somewhat for the lack of palmitoylation of the terminal cysteine residue 565, hence the increased infectivity of Ud7+Ud HA-SCS and Ud7+Ud HA-CCS over Ud7+Ud HA-SSS and the greater variability for the amount of M1 protein incorporated into released virus (or virus-like) particles. A role for palmitoylation in virus assembly has also been implicated in the assembly of VSV (37), HIV-1 (4, 32), and the alphavirus Sindbis virus (13, 37). Chemical inhibition of palmitoylation by cerulenin treatment inhibited VSV and Sindbis virus particle formation (37). In addition, site-directed mutation of palmitoylation sites in the Sindbis virus E2 (13) and HIV-1 gp41 (4) glycoproteins decreased the amount of released infectious viral particles, suggesting an important role for palmitoylation dur-

ing virus assembly. In the case of Sindbis virus, biochemical data showed that nucleocapsid binding to a synthetic, palmitoylated E2 cytoplasmic domain peptide is not sequence specific but is palmitate dependent (48). This result suggests that the nucleocapsid may specifically recognize palmitoylated E2 during the assembly of viral particles. Likewise, we hypothesize that the influenza virus HA cytoplasmic tail cysteine 565 palmitate group interacts with the matrix protein for efficient virus assembly. This interaction is likely to occur independently of lipid raft association, as a decrease in M1 TX-100 insolubility was not observed in the presence of nonpalmitoylated HA.

We also observed that the requirement for HA cytoplasmic tail palmitoylation is linked to the genotype of the M1 protein. When the WSN M gene, and most importantly the WSN M1 coding sequence, was rescued in the Ud genetic background that contained the Ud HA-SSS mutant, the recovered virus was able to replicate as efficiently as wt Ud virus. These results may explain the observations made in our previous study in which the role of palmitoylation of Ud HA was assessed in the genetic background of WSN using a helper virus rescue system (15). Rescued viruses did not exhibit a defect in protein composition, nor did they exhibit a decrease in infectivity greater than ~1 log unit in tissue culture, embryonated eggs, or mice. In the earlier study, the three conserved cysteine residues were mutated to MAY-methionine because two HA subtypes have methionine at this position instead of cysteine and tyrosine because this substitution had been previously used as a control for a normally trafficked HA protein and, thus, was thought to be tolerable at this position (6). This WSN7+Ud HA-MAY virus was able to replicate quite well. Although the presence of the WSN M1 protein may have contributed to the replication of this virus (and other viruses) in the earlier study, we also found here that the Ud HA-MAY mutation in the Ud7 genetic backbone was able to produce infectious virus without an assembly defect. Thus, tyrosine in place of palmitoylation of cysteine residue 565 may compensate for the loss of palmitate. Recently, it has been reported that the substitution of palmitoylated cysteines in the cytoplasmic domain of HIV-1 gp41 with bulky aromatic residues did not affect raft association of gp41 and these gp41 mutants were incorporated efficiently into virions (4).

Mutagenesis of the WSN (H1) HA palmitoylation sites in the WSN genetic background (WSN7+WSN HA-SSS) resulted in a virus that also grew to an intermediate level (~5×10^4 PFU/ml). These data suggest that the removal of palmitoylation sites in both H1 and H3 HA subtypes has an effect on WSN replication. However, the origin of the M1 gene appears to be important for supporting virus growth, as switching the M gene from WSN7+Ud HA-SSS to WSN6+Ud HA-SSS+Ud M further reduces virus growth to ~1×10^2 PFU/ml. The reason for the reduced growth of WSN7+WSN HA-SSS or WSN7+Ud HA-SSS compared to that of Ud6+Ud HA-SSS+WSN M is not known but likely reflects contributions from the constellation of other viral proteins. It is possible that the Ud NA or M2 proteins are critical to support efficient viral assembly and budding under nonideal conditions.

To understand further the difference between the Ud M1 protein and the WSN M1 protein on the growth of viruses that contain Ud HA-SSS, the six residues that differ between Ud M1 and WSN M1 were substituted into Ud M1 individually and in various combinations. A small increase in the titer of Ud7+Ud HA-SSS was observed when the single Ud-to-WSN M1 mutations were made. However, changing the Ud M1 protein such that it was converted to the WSN M1 amino acid sequence completely restored virus titer. When various combinations of substitutions of Ud M1 residues for WSN M1 residues were made, it was found that the alanine-to-valine mutation at position 41 and arginine-to-lysine mutation at position 95 largely restored replication to levels only ~1.5 log lower than that of Ud wt virus. The observation that the UdM-A41V M1 mutation contributed to restoring replication to the Ud7+Ud HA-SSS virus is particularly interesting, as the nature of the residue at position 41 has been implicated in influencing virus morphology (8), growth characteristics in mice (47), and adaptation of virus from the growth inhibition of the M2-specific 14C2 monoclonal antibody (12, 31, 49). Based on the available atomic structure of a fragment of the M1 protein (2, 33, 39), residue 41 is thought to be located in the membrane-binding region, making it possible that M1 protein residue 41 forms important contacts with the viral glycoproteins during assembly. The residue at position 95 (as well as residues at position 204 and 218) has also been demonstrated to promote spherical virus morphology (5, 8). In the case of the spherical WSN particles, it is possible that these residues are able to promote more efficient viral assembly and, thus, impart a decreased dependence on HA palmitoylation during assembly. The fact that all six WSN-specific residues are necessary to fully remove the dependence on HA palmitoylation for efficient virus growth suggests that a cooperative relationship exists among these residues in the M1 protein. Alternatively, the unique residues of WSN M1 may promote more efficient virus budding independently of other viral and/or cellular host factors. An understanding of how specific M1 mutations reverse the incompatibility of Ud M1 with nonpalmitoylated HA may be relevant to understanding why a restriction in free assortment between strains of influenza virus exists (38).

ACKNOWLEDGMENTS

M.T. was an associate and R.A.L. is an investigator of the Howard Hughes Medical Institute.

B.J.C. is supported by National Institutes of Health Medical Scientist Training Program grant T32 GM08152-18 and Cellular and Molecular Basis of Disease Training grant T32 GM008061-22. This work was supported in part by research grant R37 AI-20201 (R.A.L.) from the National Institutes of Allergy and Infectious Diseases.

REFERENCES

1. **Ali, A., R. T. Avalos, E. Ponimaskin, and D. P. Nayak.** 2000. Influenza virus assembly: effect of influenza virus glycoproteins on the membrane association of M1 protein. J. Virol. **74:**8709–8719.
2. **Arzt, S., F. Baudin, A. Barge, P. Timmins, W. P. Burmeister, and R. W. Ruigrok.** 2001. Combined results from solution studies on intact influenza virus M1 protein and from a new crystal form of its N-terminal domain show that M1 is an elongated monomer. Virology **279:**439–446.
3. **Bavari, S., C. M. Bosio, E. Wiegand, G. Ruthel, A. B. Will, T. W. Geisbert, M. Hevey, C. Schmaljohn, A. Schmaljohn, and M. J. Aman.** 2002. Lipid raft microdomains: a gateway for compartmentalized trafficking of Ebola and Marburg viruses. J. Exp. Med. **195:**593–602.
4. **Bhattacharya, J., P. J. Peters, and P. R. Clapham.** 2004. Human immunodeficiency virus type 1 envelope glycoproteins that lack cytoplasmic domain cysteines: impact on association with membrane lipid rafts and incorporation onto budding virus particles. J. Virol. **78:**5500–5506.
5. **Bourmakina, S. V., and A. García-Sastre.** 2003. Reverse genetics studies on the filamentous morphology of influenza A virus. J. Gen. Virol. **84:**517–527.
6. **Brewer, C. B., and M. G. Roth.** 1991. A single amino acid change in the cytoplasmic domain alters the polarized delivery of influenza virus hemagglutinin. J. Cell Biol. **114:**413–421.

7. **Cherukuri, A., R. H. Carter, S. Brooks, W. Bornmann, R. Finn, C. S. Dowd, and S. K. Pierce.** 2004. B cell signaling is regulated by induced palmitoylation of CD81. J. Biol. Chem. **279:**31973–31982.
8. **Elleman, C. J., and W. S. Barclay.** 2004. The M1 matrix protein controls the filamentous phenotype of influenza A virus. Virology **321:**144–153.
9. **Enami, M., and K. Enami.** 1996. Influenza virus hemagglutinin and neuraminidase glycoproteins stimulate the membrane association of the matrix protein. J. Virol. **70:**6653–6657.
10. **Fischer, C., B. Schroth-Diez, A. Herrmann, W. Garten, and H.-D. Klenk.** 1998. Acylation of the influenza hemagglutinin modulates fusion activity. Virology **248:**284–294.
11. **Harder, T., and M. Kuhn.** 2000. Selective accumulation of raft-associated membrane protein LAT in T cell receptor signaling assemblies. J. Cell Biol. **151:**199–208.
12. **Hughey, P. G., P. C. Roberts, L. J. Holsinger, S. L. Zebedee, R. A. Lamb, and R. W. Compans.** 1995. Effects of antibody to the influenza A virus M2 protein on M2 surface expression and virus assembly. Virology **212:**411–421.
13. **Ivanova, L., and M. J. Schlesinger.** 1993. Site-directed mutagenesis in the Sindbis virus E2 glycoprotein identify palmitoylation sites and affect virus budding. J. Virol. **67:**2546–2551.
14. **Jin, H., G. P. Leser, J. Zhang, and R. A. Lamb.** 1997. Influenza virus hemagglutinin and neuraminidase cytoplasmic tails control particle shape. EMBO J. **16:**1236–1247.
15. **Jin, H., K. Subbarao, S. Bagai, G. P. Leser, B. R. Murphy, and R. A. Lamb.** 1996. Palmitoylation of the influenza virus hemagglutinin (H3) is not essential for virus assembly or infectivity. J. Virol. **70:**1406–1414.
16. **Koegl, M., P. Zlatkine, S. C. Ley, S. A. Courtneidge, and A. I. Magee.** 1994. Palmitoylation of multiple Src-family kinases at a homologous N-terminal motif. Biochem. J. **303:**749–753.
17. **Lamb, R. A., and P. W. Choppin.** 1981. Identification of a second protein (M2) encoded by RNA segment 7 of influenza virus. Virology **112:**729–737.
18. **Lamb, R. A., and R. M. Krug.** 2001. Orthomyxoviridae: the viruses and their replication, p. 1487–1531. *In* D. M. Knipe, B. Roizman, P. M. Howley, S. E. Straus, and M. A. Martin (ed.), Fields virology, 4th ed. Lippincott, Williams & Wilkins, Philadelphia, Pa.
19. **Liu, T., and Z. Ye.** 2002. Restriction of viral replication by mutation of the influenza virus matrix protein. J. Virol. **76:**13055–13061.
20. **Luytjes, W., M. Krystal, M. Enami, J. D. Pavin, and P. Palese.** 1989. Amplification, expression and packaging of a foreign gene by influenza virus. Cell **58:**1107–1113.
21. **Melikyan, G. B., H. Jin, R. A. Lamb, and F. S. Cohen.** 1997. The role of the cytoplasmic tail region of influenza virus hemagglutinin in formation and growth of fusion pores. Virology **235:**118–128.
22. **Melkonian, K. A., A. G. Ostermeyer, J. Z. Chen, M. G. Roth, and D. A. Brown.** 1999. Role of lipid modifications in targeting proteins to detergent-resistant membrane rafts. J. Biol. Chem. **274:**3910–3917.
23. **Naeve, C. W., and D. Williams.** 1990. Fatty acids on the A/Japan/305/57 influenza virus hemagglutinin have a role in membrane fusion. EMBO J. **9:**3857–3866.
24. **Naim, H. Y., B. Amarneh, N. T. Ktistakis, and M. G. Roth.** 1992. Effects of altering palmitoylation sites on biosynthesis and function of the influenza virus hemagglutinin. J. Virol. **66:**7585–7588.
25. **Nayak, D. P., E. K.-W. Hui, and S. Barman.** 2004. Assembly and budding of influenza virus. Virus Res. **106:**147–165.
26. **Neumann, G., T. Watanabe, H. Ito, S. Watanabe, H. Goto, P. Gao, M. Hughes, D. R. Perez, R. Donis, E. Hoffmann, G. Hobom, and Y. Kawaoka.** 1999. Generation of influenza A viruses entirely from cloned cDNAs. Proc. Natl. Acad. Sci. USA **96:**9345–9350.
27. **Niwa, H., K. Yamamura, and J. Miyazaki.** 1991. Efficient selection for high-expression transfectants by a novel eukaryotic vector. Gene **108:** 193–200.
28. **Nobusawa, E., T. Aoyama, H. Kato, Y. Suzuki, Y. Tateno, and K. Nakajima.** 1991. Comparison of complete amino acid sequences and receptor-binding properties among 13 serotypes of hemagglutinins of influenza A viruses. Virology **182:**475–485.
29. **Ono, A., and E. O. Freed.** 2001. Plasma membrane rafts play a critical role in HIV-1 assembly and release. Proc. Natl. Acad. Sci. USA **98:**13925–13930.
30. **Philipp, H. C., B. Schroth, M. Veit, M. Krumbiegel, A. Herrmann, and M. F. G. Schmidt.** 1995. Assessment of fusogenic properties of influenza virus hemagglutinin deacylated by site-directed mutagenesis and hydroxylamine treatment. Virology **210:**20–28.
31. **Roberts, P. C., R. A. Lamb, and R. W. Compans.** 1998. The M1 and M2 proteins of influenza A virus are important determinants in filamentous particle formation. Virology **240:**127–137.
32. **Rousso, I., M. B. Mixon, B. K. Chen, and P. S. Kim.** 2000. Palmitoylation of the HIV-1 envelope glycoprotein is critical for viral infectivity. Proc. Natl. Acad. Sci. USA **97:**13523–13525.
33. **Ruigrok, R. W., A. Barge, P. Durrer, J. Brunner, K. Ma, and G. R. Whittaker.** 2000. Membrane interaction of influenza virus M1 protein. Virology **267:**289–298.
34. **Sakai, T., R. Ohuchi, and M. Ohuchi.** 2002. Fatty acids on the A/USSR/77 influenza virus hemagglutinin facilitate the transition from hemifusion to fusion pore formation. J. Virol. **76:**4603–4611.
35. **Sarkar, D. P., S. J. Morris, O. Eidelman, J. Zimmerberg, and R. Blumenthal.** 1989. Initial stages of influenza hemagglutinin-induced cell fusion monitored simultaneously by two fluorescent events: cytoplasmic continuity and lipid mixing. J. Cell Biol. **109:**113–122.
36. **Scheiffele, P., A. Rietveld, T. Wilk, and K. Simons.** 1999. Influenza viruses select ordered lipid domains during budding from the plasma membrane. J. Biol. Chem. **274:**2038–2044.
37. **Schlesinger, M. J., and C. Malfer.** 1982. Cerulenin blocks fatty acid acylation of glycoproteins and inhibits vesicular stomatitis and Sindbis virus particle formation. J. Biol. Chem. **257:**9887–9890.
38. **Scholtissek, C., J. Stech, S. Krauss, and R. G. Webster.** 2002. Cooperation between the hemagglutinin of avian viruses and the matrix protein of human influenza A viruses. J. Virol. **76:**1781–1786.
39. **Sha, B., and M. Luo.** 1997. Structure of a bifunctional membrane-RNA binding protein, influenza virus matrix protein M1. Nat. Struct. Biol. **4:** 239–244.
40. **Simons, K., and D. Toomre.** 2000. Lipid rafts and signal transduction. Nat. Rev. Mol. Cell Biol. **1:**31–41.
41. **Simpson, D. A., and R. A. Lamb.** 1992. Alterations to influenza virus hemagglutinin cytoplasmic tail modulate virus infectivity. J. Virol. **66:**790–803.
42. **Steinhauer, D. A., S. A. Wharton, D. C. Wiley, and J. J. Skehel.** 1991. Deacylation of the hemagglutinin of influenza A/Aichi/2/68 has no effect on membrane fusion properties. Virology **184:**445–448.
43. **Takeda, M., G. P. Leser, C. J. Russell, and R. A. Lamb.** 2003. Influenza virus hemagglutinin concentrates in lipid raft microdomains for efficient viral fusion. Proc. Natl. Acad. Sci. USA **100:**14610–14617.
44. **Takeda, M., A. Pekosz, K. Shuck, L. H. Pinto, and R. A. Lamb.** 2002. Influenza A virus M2 ion channel activity is essential for efficient replication in tissue culture. J. Virol. **76:**1391–1399.
45. **Veit, M., E. Kretzschmar, K. Kuroda, W. Garten, M. F. G. Schmidt, H.-D. Klenk, and R. Rott.** 1991. Site-specific mutagenesis identifies three cysteine residues in the cytoplasmic tail as acylation sites of influenza virus hemagglutinin. J. Virol. **65:**2491–2500.
46. **Wagner, R., A. Herwig, N. Azzouz, and H.-D. Klenk.** 2005. Acylation-mediated membrane anchoring of avian influenza virus hemagglutinin is essential for fusion pore formation and virus infectivity. J. Virol. **79:**6449–6458.
47. **Ward, A. C.** 1995. Specific changes in the M1 protein during adaptation of influenza virus to mouse. Arch. Virol. **140:**383–389.
48. **Wilkinson, T. A., T. L. Tellinghuisen, R. J. Kuhn, and C. B. Post.** 2005. Association of Sindbis virus capsid protein with phospholipid membranes and the E2 glycoprotein: implications for alphavirus assembly. Biochemistry **44:**2800–2810.
49. **Zebedee, S. L., and R. A. Lamb.** 1989. Growth restriction of influenza A virus by M2 protein antibody is genetically linked to the M1 protein. Proc. Natl. Acad. Sci. USA **86:**1061–1065.
50. **Zhang, J., G. P. Leser, A. Pekosz, and R. A. Lamb.** 2000. The cytoplasmic tails of the influenza virus spike glycoproteins are required for normal genome packaging. Virology **269:**325–334.
51. **Zhang, J., A. Pekosz, and R. A. Lamb.** 2000. Influenza virus assembly and lipid raft microdomains: a role for the cytoplasmic tails of the spike glycoproteins. J. Virol. **74:**4634–4644.
52. **Zhirnov, O. P., T. E. Konakova, W. Garten, and H.-D. Klenk.** 1999. Caspase-dependent N-terminal cleavage of influenza virus nucleocapsid protein in infected cells. J. Virol. **73:**10158–10163.
53. **Zurcher, T., G. Luo, and P. Palese.** 1994. Mutations at palmitoylation sites of the influenza virus hemagglutinin affect virus formation. J. Virol. **68:** 5748–5754.